Catena 199 (2021) 105098

Contents lists available at ScienceDirect

Catena

journal homepage: www.elsevier.com/locate/catena

Three-dimensional quantification of soil pore structure in wind-deposited loess under different vegetation types using industrial X-ray computed tomography

Jiangbo Qiao [a], Xingting Liu [a], Yuanjun Zhu [a], Xiaoxu Jia [b], Ming'an Shao [a,b,c,*]

[a] State Key Laboratory of Soil Erosion and Dryland Agriculture on the Loess Plateau, Northwest A&F University, Yangling 712100, China
[b] Key Laboratory of Ecosystem Network Observation and Modeling, Institute of Geographic Sciences and Natural Resources Research, Chinese Academy of Sciences, Beijing 100101, China
[c] College of Resources and Environment, University of Chinese Academy of Sciences, Beijing 100190, China

ARTICLE INFO

Keywords:
Deep profile
Soil structure
Vegetation type
X-ray computed tomography

ABSTRACT

Quantifying the soil pore structure is critical for understanding plant growth and water/solute movements in the soil. However, most previous studies quantified the soil pore structure in a shallow layer by using low resolution medical computed tomography (CT), whereas few have quantified the soil pore structure in deep soil layers with high resolution CT. In this study, we quantified the soil pore structure of wind-deposited loess under different vegetation types (wheat, weeds, apple orchard, and *Robinia pseudoacacia*) at depths from 0 to 4.5 m by industrial CT. The results showed that the soil pore number and porosity tended to decreased with depth, but there were no significance differences below 2 m among all vegetation types. For different depths and vegetation types, the number of pores measuring 0–100 μm was highest, followed by those measuring.

100–500 μm, and lowest for those measuring > 1000 μm. The contribution of pores measuring 100–500 μm to the total pore volume was highest. The variations in the connectivity and surface area density were also focused mainly within the depth down to 2 m, and the variations were minor below 2 m. There were no significant differences in the bulk density and soil pore characteristics under different vegetation types, except for weeds. The results obtained in this study provide insights into the interactions between vegetation and soil water, as well as the hydrological processes for the wind-deposited loess.

1. Introduction

The soil pore structure refers to the shape, size, and spatial distribution of soil pores, including the quantitative and morphological characteristics of pores, pore number, pore diameter, pore size distribution, roundness rate, and spatial distribution characteristics in terms of the connectivity, junction density, and branch density (Cheng et al., 2012). The soil pore structure directly affects the migration route and mode for water in the soil, and it has strong relationships with surface runoff and the permeability of soil (Poesen and Ingelmo-Sanchez 1992), as well as influencing soil fertility (Edwards et al., 1988). Therefore, quantifying the soil pore structure is very important for understanding the transport of water and solutes in the soil.

Many methods can be used to quantify the soil pore structure, including dye tracing (Sander and Gerke, 2007), soil water retention curves (Głąb et al., 2013), mercury intrusion curves (Dim et al., 2016), and X-ray computed tomography (CT) (Li et al., 2002; Li et al., 2016). The CT method is effective for measuring the pore number, size, shape, connectivity, and other characteristics to obtain the complete three-dimensional (3D) structure, so this method has been applied widely to study the pore structure of soils (Pierret et al., 2002; Hu et al., 2016). For example, Wang et al. (2019) applied X-ray CT to assess the effects of a land use change from growing rice to vegetables on the soil structure quality, and found a significant correlation between degradation of the soil structure and a decrease in the soil organic matter content. Zhang et al. (2014) analyzed the cracks in two paddy soils formed by alternate flooding and drying cycles to assess their impacts on preferential flow, and showed that the paddy soil cracks could improve the infiltration of water, but their effect on the preferential flow was minor below the plow pan. In addition, Kochiieru et al. (2018) investigated the effects of the

* Corresponding author at: State Key Laboratory of Soil Erosion and Dryland Agriculture on the Loess Plateau, Northwest A&F University, Yangling 712100, China.
E-mail address: shaoma@igsnrr.ac.cn (M. Shao).

https://doi.org/10.1016/j.catena.2020.105098
Received 19 October 2020; Received in revised form 8 December 2020; Accepted 9 December 2020
Available online 23 December 2020

soil macroporosity on CO_2 efflux in soils with different origins and land management practices by using X-ray CT, and found that the amount of macropores and the macropore geometry were important factor that influenced the CO_2 flow.

The Loess Plateau of China has the most widespread distribution and thickest layer of wind-deposited loess area throughout the world, and two-thirds of this region is classified as arid or semiarid (Liu, 1985). Due to the lack of water resources and great depth of the groundwater, there are strong interactions between the soil, vegetation, and water. Quantifying soil pore structure is helpful for understanding the relationships between vegetation, water, and hydrological processes in the loess. Previous studies have investigated the soil pore characteristics under different vegetation types on the Loess Plateau (Zhao et al., 2010; Li et al. 2016). However, these studies generally employed medical CT systems with low resolution where they mainly detected macropores (>1 mm), and the depth of the CT scans was confined to the shallow layers (<50 cm). Therefore, the soil pore structure in the deep soil layers under different vegetation types should be assessed using high resolution CT.

Therefore, the objectives of this study were: (i) to reconstruct the 3D structure of soil pores in the deep soil layer (0–5 m) under different vegetation types in the Loess Plateau region of China by using high resolution industrial CT; (ii) to quantify the two-dimensional (2D) and 3D soil pore structure characteristics; and (iii) to determine the relationships between the soil pore structure and soil physicochemical properties.

2. Materials and methods

2.1. Study area description

This study was conducted at Wangdonggou watershed, Xianyang City, Shaanxi Province, which is located on the Loess Plateau in south China (N35°12′N, E107°40′E) (Fig. 1), and it is a typical plateau gully area. This area has a continental climate with a mean annual temperature of 9.1 °C and mean annual precipitation of 580 mm. Typical dryland rain-fed agriculture is conducted in the study area. The soil texture is silt loam and the soil type is classified as Ustoll according to the USDA taxonomy, where the parent material is deep loamy Malan loess (Li et al., 1985). The Loess Plateau is located in the East Asian monsoon climate region and it has experienced 37 alternating dry and wet climatic cycles in the past 2.5 million years (Ding et al., 1989). Yellow paleosol alternates with reddish brown paleosol in the soil layer (Zhao et al., 2002).

2.2. Soil sampling

Four areas with different vegetation types were selected as sampling sites, where the main vegetation comprised wheat, weeds (*Stipa bungeana* Trin.), an apple orchard, and *Robinia pseudoacacia*. Given the deep roots of the apple and *Robinia pseudoacacia* trees, and the difficulty of digging holes manually, we selected 4.5 m as the sampling depth. In addition, CT scanning was expensive so we collected undisturbed soil samples at intervals of 1 m. Manual excavation was conducted to collect soil samples at depths of 0.5 m, 1.5 m, 2.5 m, 3.5 m, and 4.5 m. The undisturbed soil cores were collected in polyvinylchloride cylinders (diameter: 3.5 cm, length: 5 cm) for CT scans, and metal cylinders (diameter: 5 cm, length: 5 cm) to measure the bulk density. We collected three undisturbed soil cores as replicates for each depth at three different locations. The corresponding disturbed soil samples were also collected at the same position. In total, 60 undisturbed soil samples were collected for CT scanning and 60 disturbed soil samples for measuring the physical and chemical properties.

The disturbed soil samples were air dried, separated, and passed

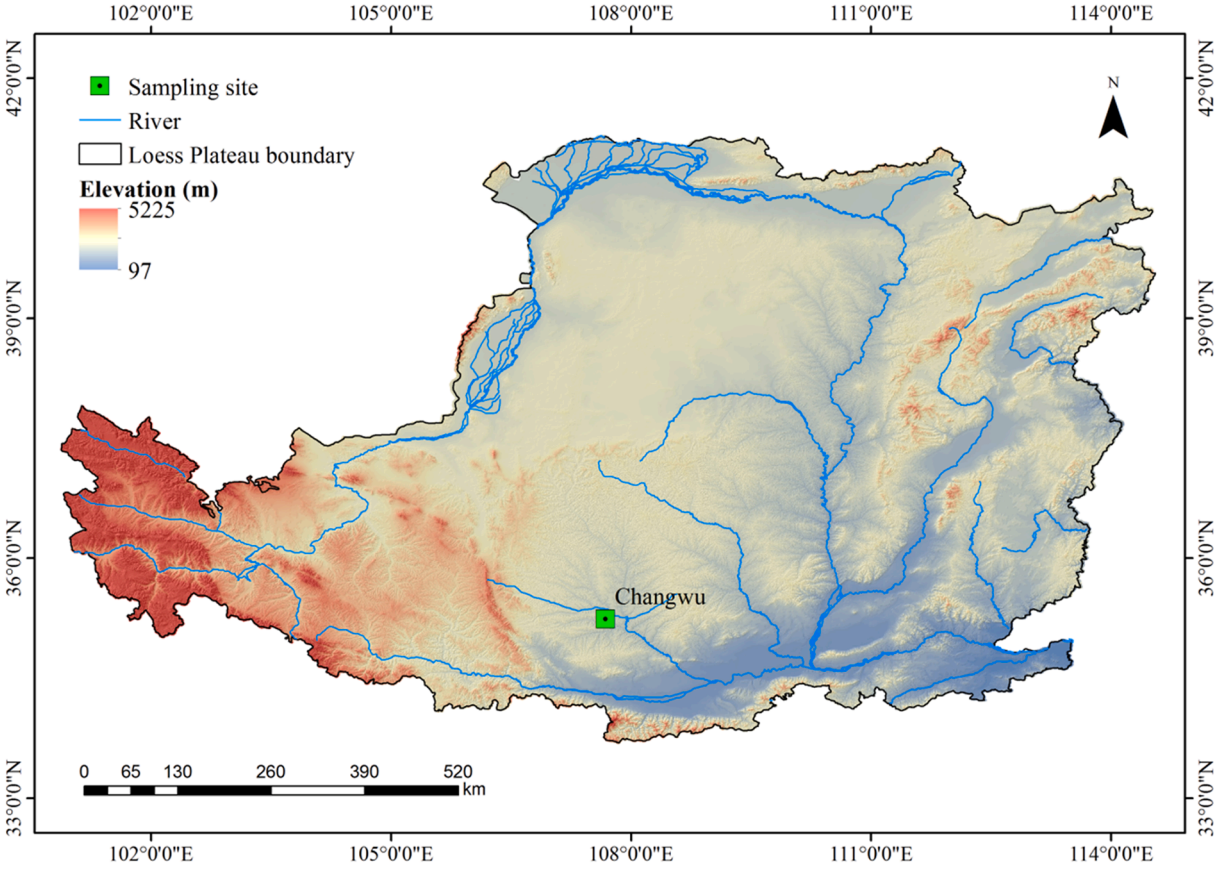

Fig. 1. Location of the sampling site in the Loess Plateau region of China.

through a 0.25-mm mesh. The SOC contents of the soil samples that passed through 0.25-mm sieves were determined using the dichromate oxidation method (Nelson and Sommers, 1982). The bulk density was measured based on the volume–mass relationship for each oven-dried core sample.

2.3. CT scanning and image analysis

The undisturbed soil cores were scanned at an energy level of 70 kV and current of 80 μA using a GE Phoenix Industrial X-ray CT scanner (Nanotom® S) at the Institute of Soil Science, Chinese Academy of Sciences, Nanjing, China. After scanning, 2303 slices were produced in a horizontal view for each sample.

The scanned images were analyzed with ImageJ software (version 1.48) and the ImageJ plugin BoneJ (Doube et al., 2010). First, a volume comprising 10 mm × 10 mm × 25 mm was selected from each core data. Second, voids near the core walls were excluded to minimize the effects of beam hardening (Schneider et al., 2012) and any image noise was reduced by a median filter. Third, a reasonable threshold value was determined by selecting the maximum inter-class entropy (Jassogne

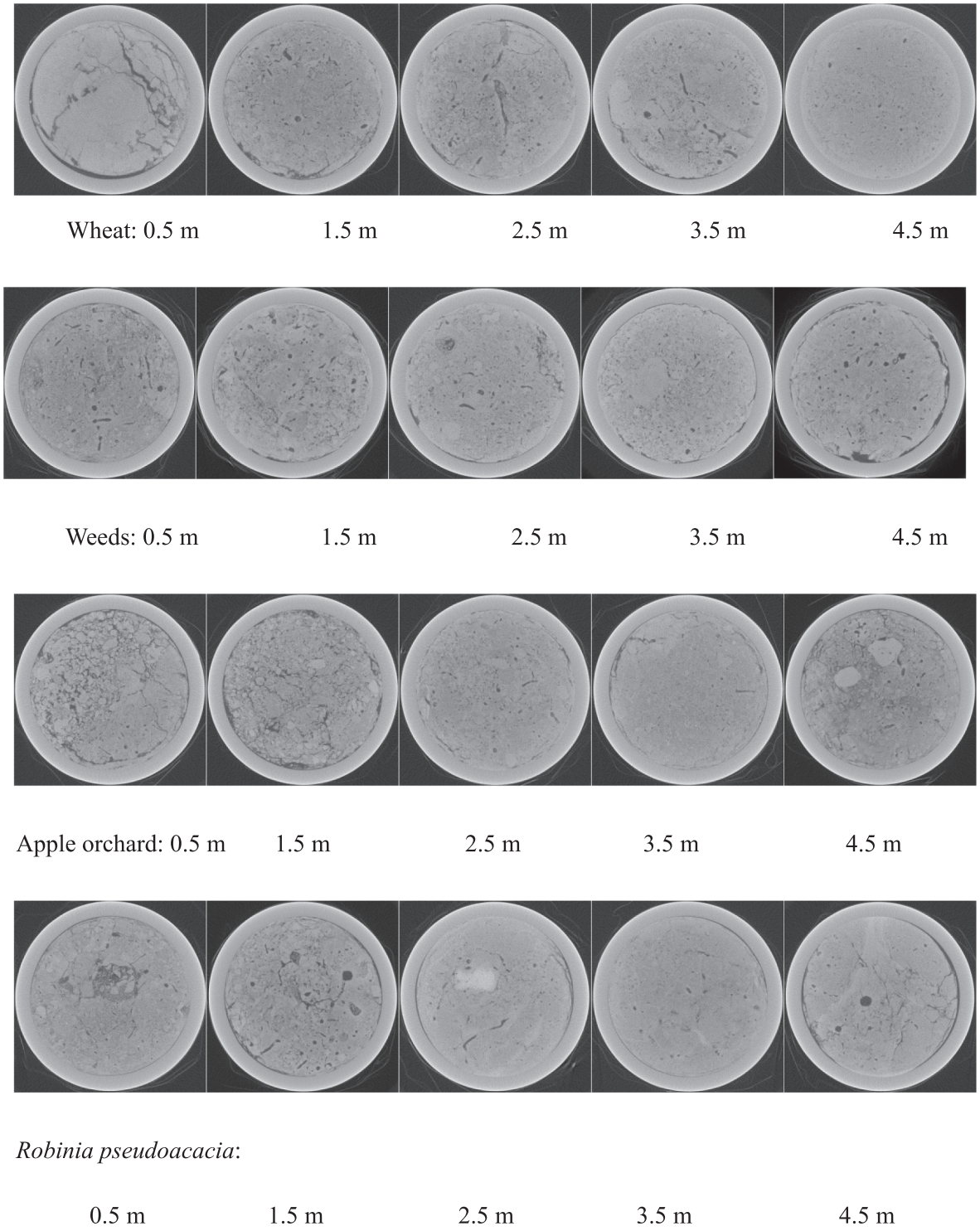

Fig. 2. Detailed two-dimensional grayscale images obtained at different depths under various vegetation types. Pores are shown in black and solid particles in grey.

et al., 2010), which was checked by visual inspection (Luo et al., 2010). Subsequently, image analysis was conducted using the processed binary images. Finally, the 2D pore characteristics were calculated with the particle analysis tool and a 3D visualization was constructed using the saturated volume rendering method in ImageJ.

2.4. Statistical analyses

One-way analysis of variance was conducted to detect differences in the soil pore characteristics at various depths and under different vegetation types based on the least significant difference method. Pearson's correlation coefficients were calculated to assess the correlations between the pore characteristics and the soil physicochemical

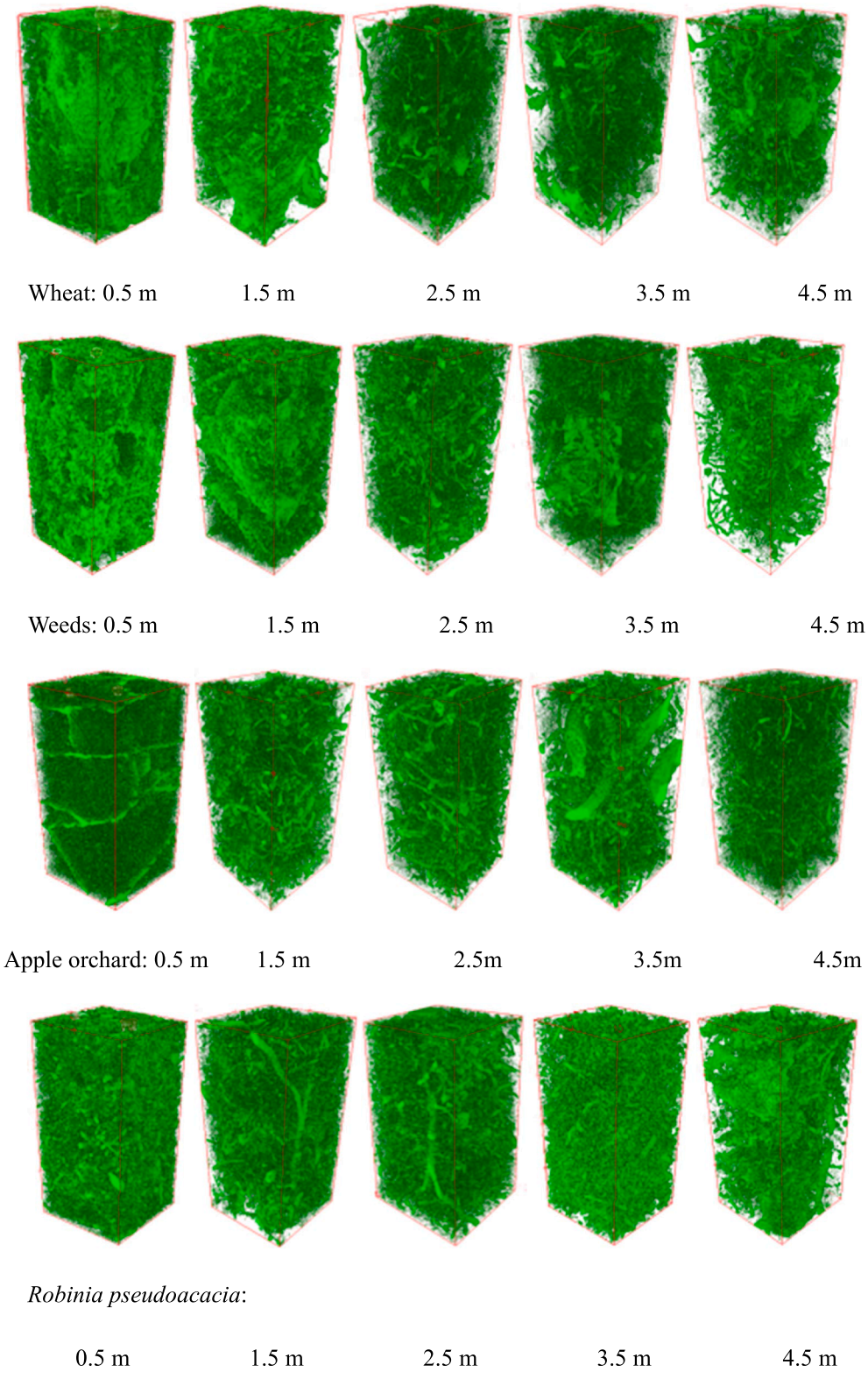

Fig. 3. Three-dimensional visualizations of the soil pore networks (10 mm × 10 mm × 25 mm) at different depths under various vegetation types.

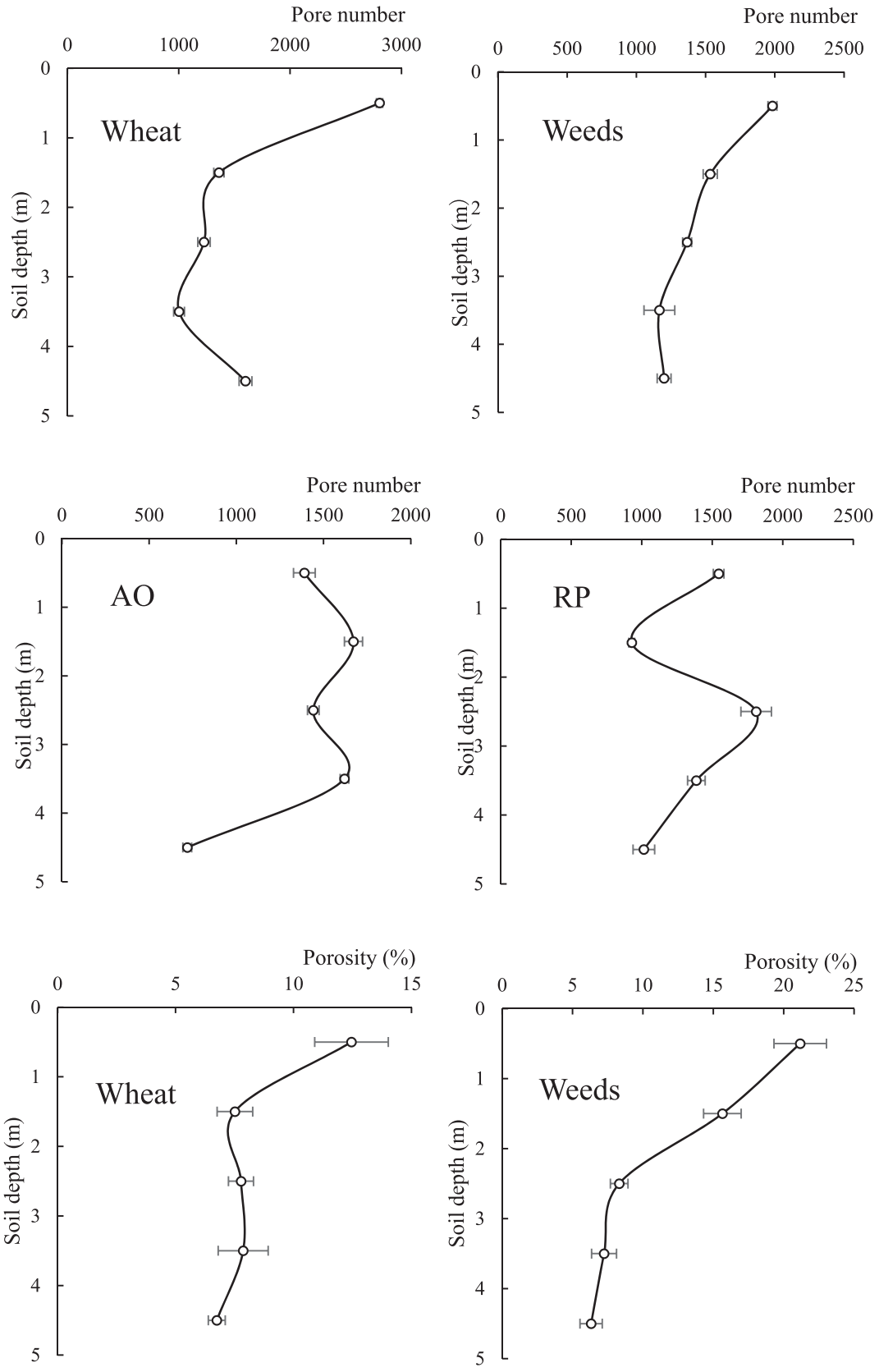

Fig. 4. Two-dimensional characteristics of soil macropores at different depths under various vegetation types. AO, apple orchard; RP, *Robinia pseudoacacia.* Values are the mean ± standard error.

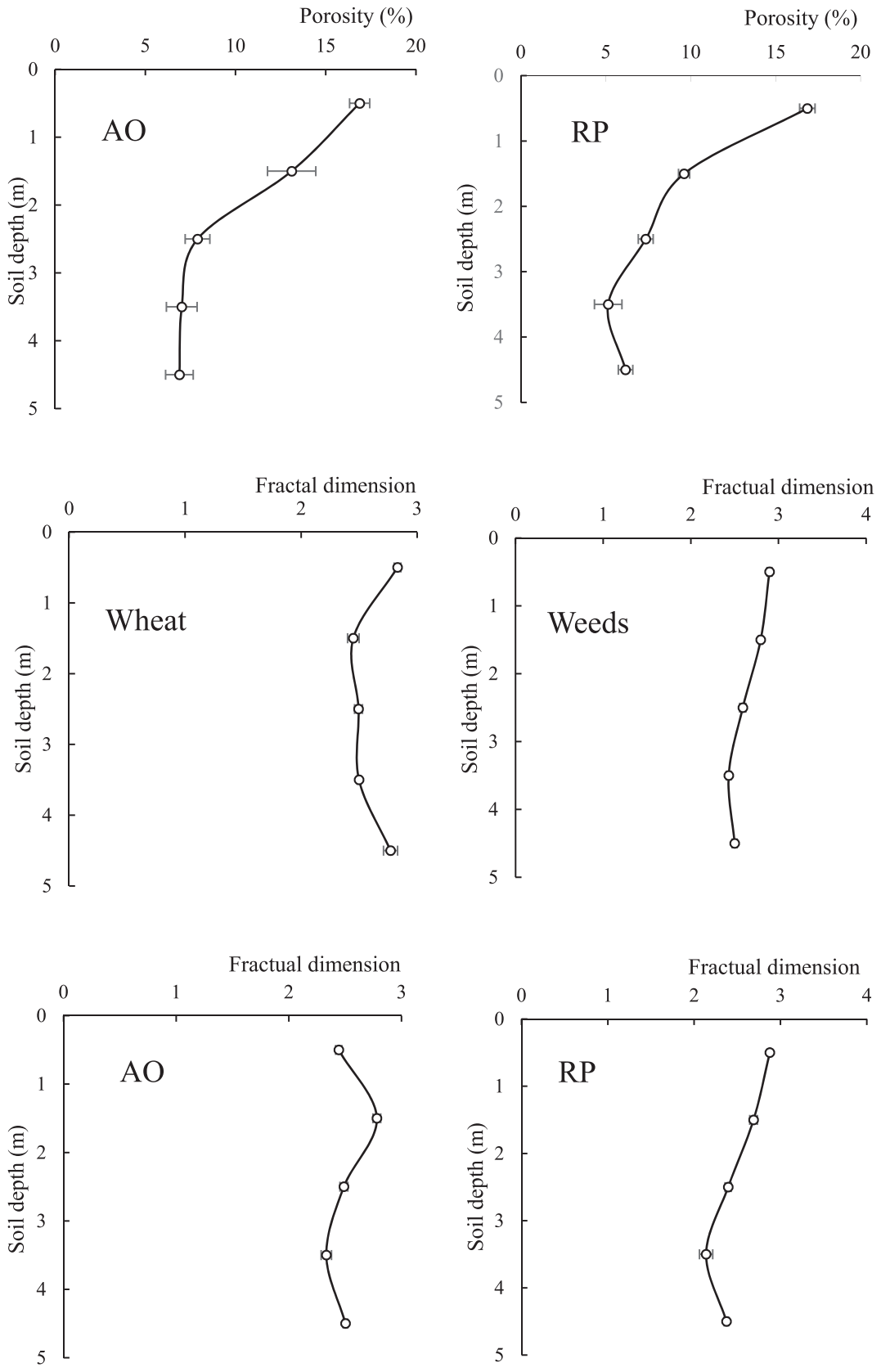

Fig. 4. (*continued*).

properties. Statistically significant differences were accepted at the $P < 0.05$ and $P < 0.01$ levels. All statistical analyses were conducted using Statistical Product and Service Solutions (SPSS) software (version 13.0).

Results

2.5. Visualization of pore characteristics at different depths and under various vegetation types

Fig. 2 shows the 2D slices obtained at different depths and under various vegetation types, where the scans were acquired from the middle of each soil sample. Under wheat and weeds, the pore number and

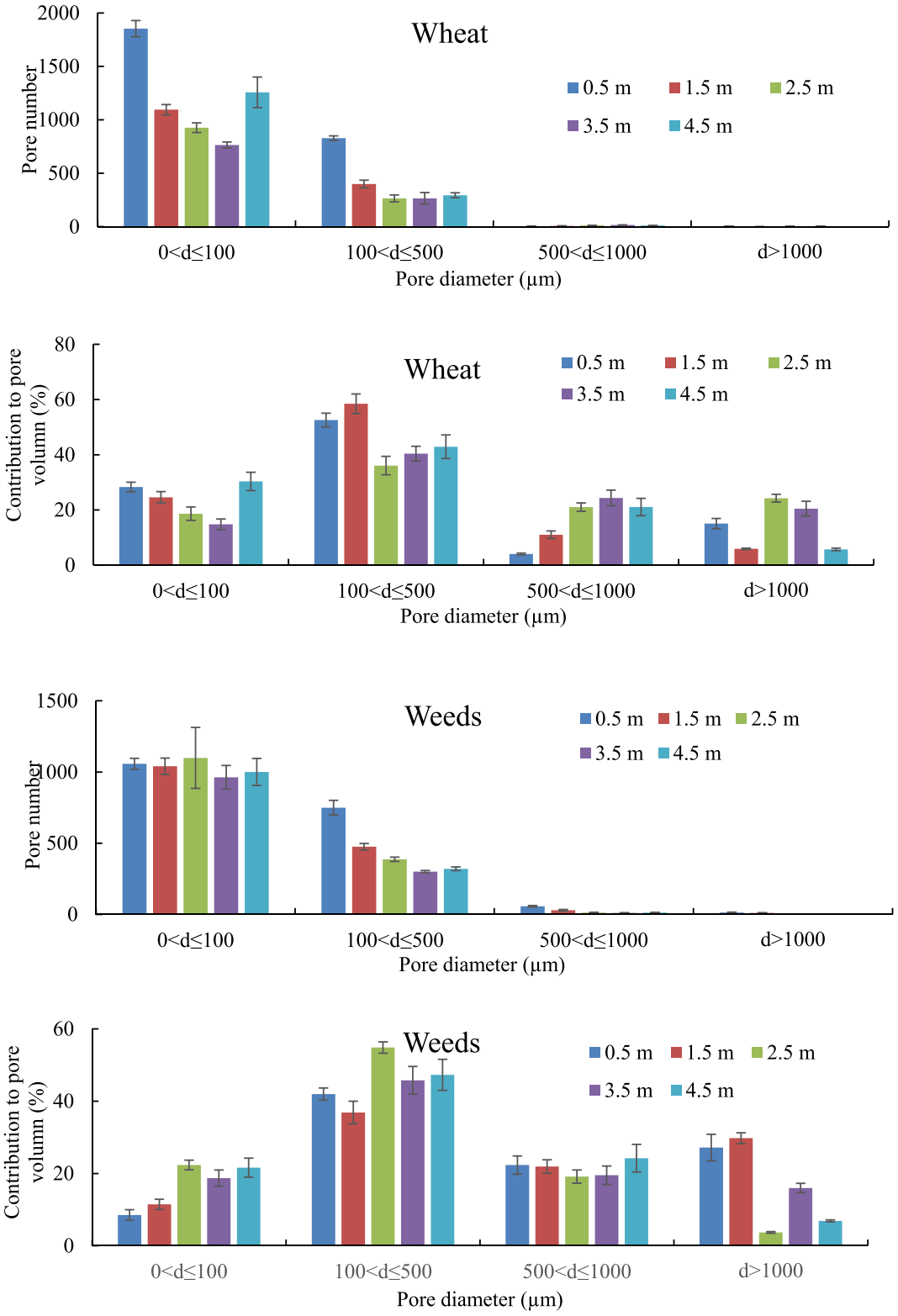

Fig. 5. Pore size distributions and contributions of pores with each size to the total pore volume. AO, apple orchard; RP, *Robinia pseudoacacia.* Values are the mean ± standard error.

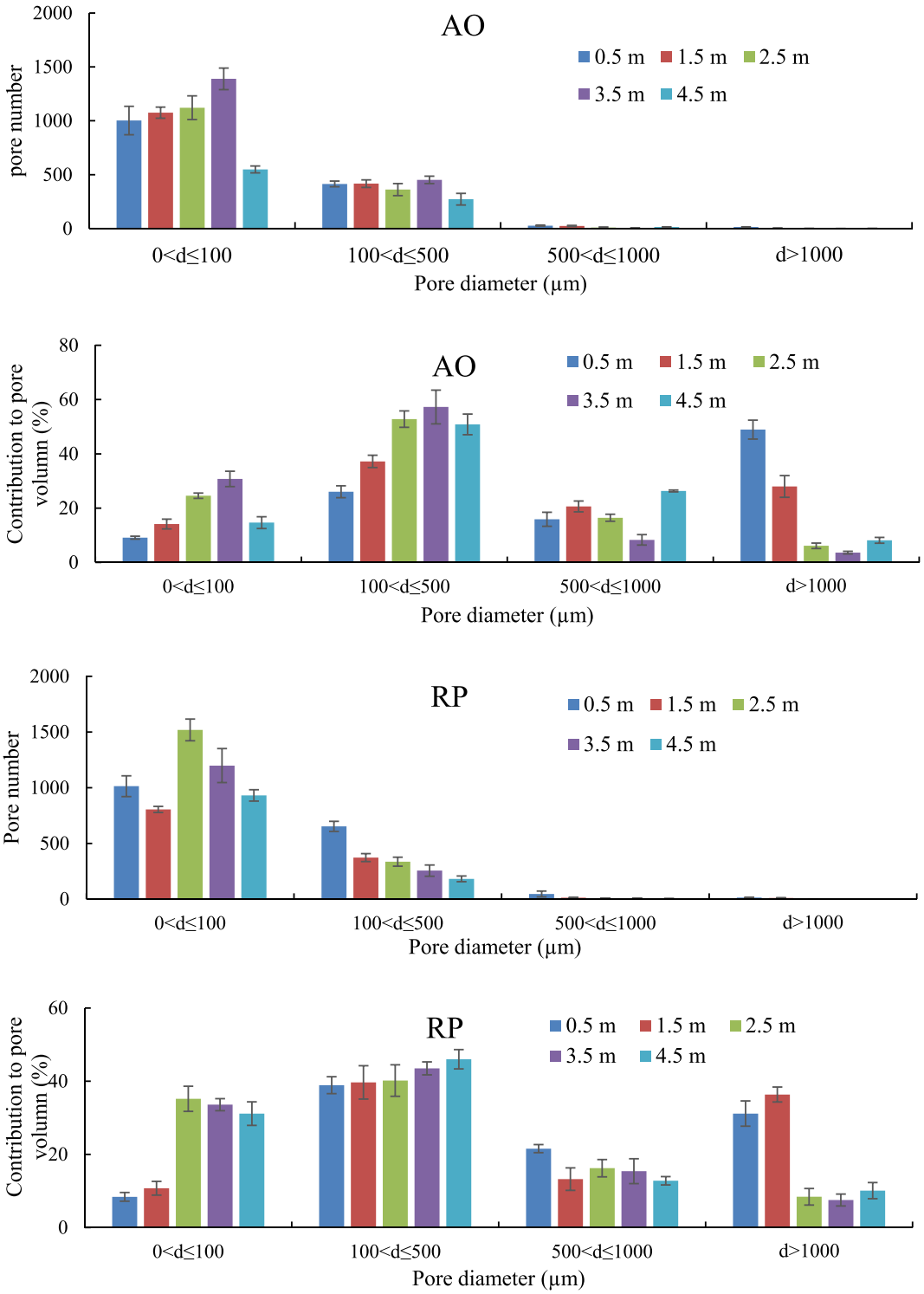

Fig. 5. (*continued*).

pore size were higher at 0.5 m than those at 1.5 m, 2.5 m, 3.5 m, and 4.5 m. Under *Robinia pseudoacacia* and apples, the pore number and pore size were higher at 0.5 m and 1.5 m than those at 2.5 m, 3.5 m, and 4.5 m. These differences may be explained by *Robinia pseudoacacia* and apple trees having deeper roots than wheat and weeds. In addition, the 3D visualizations of the pore characteristics showed that the pore networks were more complex and not isolated at depths of 0.5 m and 1.5 m under Robinia pseudoacacia and apples compared with those at other depths, and the pore networks of 0.5 m under wheat and weeds got the same results (Fig. 3).

2.6. Variations in pore number, porosity, and fractal dimension (D)

Fig. 4 shows the 2D characteristics (pore number, porosity, and D) of the soil pores at different depths under various vegetation types. In general, the number of pores tended to decrease throughout the profile under all four vegetation types, but the distribution characteristics differed. For example, the distribution characteristic of the number of

pores under wheat tended to decrease and then increase, whereas a fluctuating curve was obtained under apples. In addition, the porosity of the soil under all four vegetation types tended to decrease as the depth increased. However, there were no significant differences in the macroporosity at 2.5 m, 3.5 m, and 4.5 m under *Robinia pseudoacacia* and apples ($P > 0.05$), but there were no significant differences in the

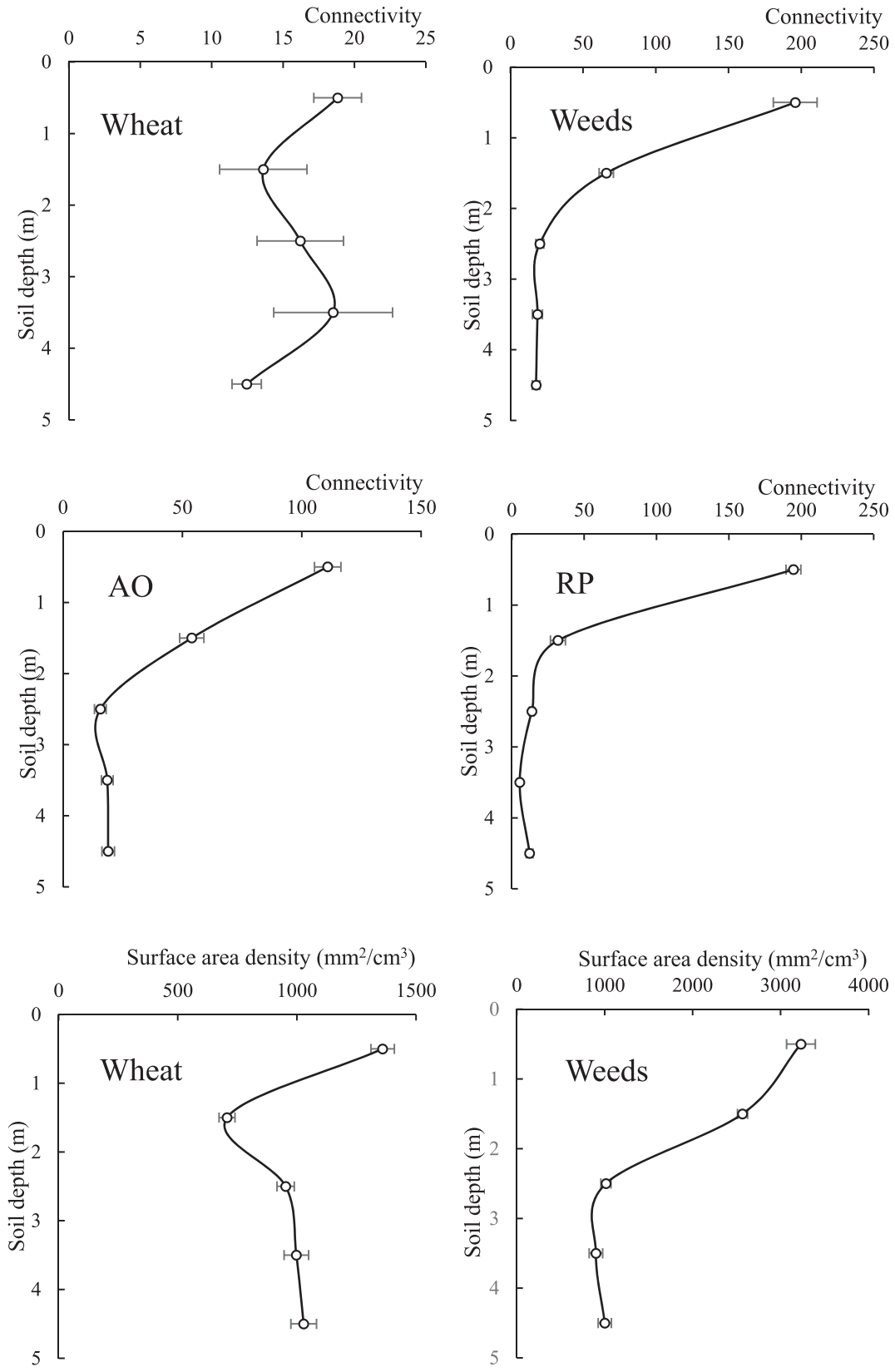

Fig. 6. Connectivity and surface area density of soil macropores at different depths under various vegetation types. AO, apple orchard; RP, *Robinia pseudoacacia.* Values are the mean ± standard error.

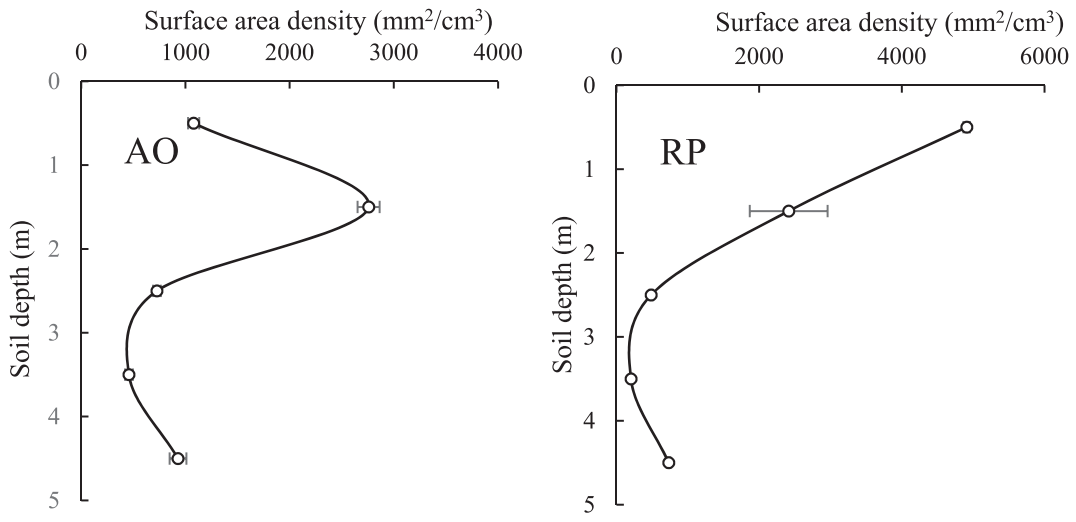

Fig. 6. (*continued*).

porosity at 1.5 m, 2.5 m, 3.5 m, and 4.5 m under wheat and weeds ($P > 0.05$). The fractal dimension D did not differ according to any regular pattern among the four vegetation types.

In order to assess the soil pore distribution characteristics in more detail, we quantified the number of pores with different sizes and their contributions to the total pore volume (Fig. 5). The number of pores measuring 0–100 μm was highest, followed by those measuring 100–500 μm, and then those measuring > 1000 μm at different depths and under various vegetation types (Fig. 5). In addition, the number of pores with different pore sizes tended to decrease to varying extents as the depth increased. The number of pores that measured 0–100 μm was highest but their contribution to the total pore volume was low. In addition, the contribution of the pores that measured 100–500 μm to the total pore volume was the highest among the four vegetation types. It should be noted that the contribution of the pores that measured > 1000 μm to the total pore volume was similar to that of the pores that measured 100–500 μm at 0.5 m and 1.5 m under *Robinia pseudoacacia* and apples. *Robinia pseudoacacia* and apple trees have deeper roots, thereby leading to more pores measuring > 1000 μm, and thus they made a greater contribution to the total pore volume.

2.7. Variations in connectivity of pores and surface area density (SAD)

Fig. 6 shows the connectivity and SAD at different depths under various vegetation types. The connectivity tended to be similar under the four vegetation types, where it decreased initially and then remained stable below 2 m. Thus, the variations in the connectivity mainly occurred in the top 2 m and the variations were small below 2 m, which was similar to the trend found in the porosity. Similar to the pore number, SAD generally tended to decrease under the four vegetation types but the distribution characteristics differed. In addition, it should be noted that there were no significant differences in the connectivity and SAD at 2.5 m, 3.5 m, and 4.5 m under the four vegetation types.

2.8. Relationships between soil pore characteristics and physicochemical properties

In order to determine the factors that influenced the soil pore structure, we calculated the relationships between the soil pore characteristics and soil physicochemical properties (bulk density and SOC) (Table 1) under the different vegetation types (Table 2). There were no significance differences in the bulk density and soil pore characteristics under *Robinia pseudoacacia*, apples, and wheat ($P > 0.05$), but the bulk density had a significant negative relationship with the pore characteristics under weeds ($P < 0.05$). There were no significance differences between the SOC and soil pore characteristics under wheat, weeds, and apples ($P > 0.05$), but there was a significant positive relationship between SOC and the pore characteristics (except for the macropore number) under *Robinia pseudoacacia* ($P < 0.05$). These results indicate that the bulk density and SOC did not have important effects on the soil pore characteristics at depths from 0 to 4.5 m.

3. Discussion

3.1. Effects of bulk density and SOC on the soil pore characteristics

The bulk density is considered an important variable that influences the soil pore structure (Feng et al., 2018; Mahmoodlu et al. 2016). Feng et al. (2020) employed CT to quantify the 3D structure of macropore networks in different soils compacted to a bulk density of 1.3–1.8 g cm^{-3} and found that the macropore size and macroporosity decreased significantly as the soil compaction increased. In the present study, we found that the bulk density under different vegetation types ranged among 1.31–1.39, 1.27–1.50, 1.31–1.37, and 1.31–1.41 g cm^{-3} at depths of 0.5 m, 1.5 m, 2.5 m, 3.5 m, and 4.5 m throughout the profile, respectively, and thus the variations were low and the bulk density had no significant correlations with the soil pore characteristics. Therefore,

Table 1
Bulk density (BD) and soil organic matter (SOC) of different vegetation types for different depth.

	Wheat		Weeds		Apple orchard		Robinia pseudoacacia.	
Depth (m)	BD (g/cm^{-3})	SOC (g/kg)	BD (g/cm^{-3})	SOC (g/kg)	BD (g/cm^{-3})	SOC (g/kg)	BD (g/cm^{-3})	SOC (g/kg)
0.5	1.31 ± 0.007	3.68 ± 0.011	1.27 ± 0.004	3.68 ± 0.053	1.38 ± 0.014	5.62 ± 0.015	1.32 ± 0.016	4.44 ± 0.011
1.5	1.32 ± 0.017	2.97 ± 0.002	1.37 ± 0.009	2.97 ± 0.038	1.32 ± 0.015	6.94 ± 0.040	1.35 ± 0.006	3.4 ± 0.009
2.5	1.36 ± 0.003	4.69 ± 0.045	1.44 ± 0.018	4.69 ± 0.045	1.31 ± 0.009	4.88 ± 0.048	1.38 ± 0.015	2.36 ± 0.045
3.5	1.40 ± 0.008	3.77 ± 0.064	1.51 ± 0.017	3.77 ± 0.064	1.35 ± 0.009	4.16 ± 0.050	1.37 ± 0.004	1.83 ± 0.017
4.5	1.36 ± 0.006	1.96 ± 0.016	1.48 ± 0.025	1.96 ± 0.046	1.34 ± 0.008	5.33 ± 0.032	1.42 ± 0.007	1.96 ± 0.007

BD, bulk density; SOC, soil organic content. Values are the mean ± standard error.

Table 2
Correlation coefficients between bulk density (BD) and soil organic carbon (SOC) with soil pore characteristics under different vegetation types.

Vegetation type	Variable	Depth	Count	%Area	D	Connectivity	SAD
Weeds	BD	0.787	–0.732	–0.564	–0.360	0.187	–0.182
	SOC	–0.773	0.844	0.716	0.518	–0.161	0.457
Wheat	BD	0.852	–0.936*	–0.898*	–0.968**	–0.846	–0.899*
	SOC	–0.409	0.191	0.101	0.083	0.093	–0.029
Apple orchard	BD	–0.276	–0.165	0.492	–0.530	0.682	–0.331
	SOC	–0.516	0.108	0.618	0.93	0.464	0.954
Robinia pseudoacacia	BD	0.962**	–0.236	–0.836	–0.747	–0.775	–0.831
	SOC	–0.933*	0.067	0.971**	0.964**	0.891*	0.977**

D, fractal dimension; SAD, surface area density.
* Significant difference at 0.05 level
** Significant difference at 0.01 level

the bulk density affected the pore characteristics only within certain ranges. In addition, SOC is considered to influence the soil pore structure (Dal Ferro et al., 2013; Xu et al., 2018). However, previous studies found that the SOC was mainly present in the shallow layer, where the SOC contents were high and they varied greatly. By contrast, in the present study, the SOC contents were mainly detected in the deep soil layer and they varied little, and thus they had no influence on the soil pore characteristics.

3.2. Effects of different vegetation types on soil pore characteristics

Plant roots affect the soil pore structure via mechanical intercalation and by squeezing the surrounding soil during the intercalation process (Sun et al., 2015). Clearly, the roots differ among vegetation types. In the present study, apple and *Robinia pseudoacacia* trees had deeper and more developed roots, whereas wheat and weeds had shallow and underdeveloped roots. In addition, the number of roots gradually decreases as the depth increases. In the present study, we found that the variations in the 2D and 3D soil pore characteristics under different vegetation types occurred mainly in the 2 m layer. Thus, although the *Robinia pseudoacacia* and apple trees had deeper roots, the effects of their roots on the soil pore characteristics were mainly focused within the top 2 m layer.

4. Conclusions

In this study, we quantified the soil pore structure (pore number, porosity, D, connectivity, and SAD) at depths from 0 to 4.5 m under different vegetation types (wheat, weeds, apple orchard, and *Robinia pseudoacacia*) by using industrial CT. The results showed that the pore number, porosity, connectivity, and SAD all decreased as the depth increased, but they did not differ significantly among the vegetation types below 2 m. The number of pores measuring 0–100 μm was highest and the number of those measuring > 1000 μm was lowest. In addition, pores that measured 100–500 μm made the greatest contribution to the total pore volume under all four vegetation types. The bulk density and SOC did not have important effects on the soil pore characteristics at depths from 0 to 5 m. Our results provide insights into the effects of vegetation and water on the soil structure and hydrological processes.

Declaration of Competing Interest

The authors declare that they have no known competing financial interests or personal relationships that could have appeared to influence the work reported in this paper.

Acknowledgments

This study was supported by the Strategic Priority Research Program of Chinese Academy of Sciences (XDB40000000), and the Postdoctoral Special Funding (2019TQ0266). The authors thank the editor and reviewers for their valuable comments and suggestions.

References

Cheng, Y.N., Liu, J.L., Zhang, J.B., 2012. Advance in the Study on Quantification of Soil Pore Structure. Chin. J. Soil Sci. 43 (04), 988–994.
Dal Ferro, N., Charrier, P., Morari, F., 2013. Dual-scale micro-CT assessment of soil structure in a long-term fertilization experiment. Geoderma 204–205, 84–93.
Dim, P.E., Fletcher, R.S., Rigby, S.P., 2016. Improving the accuracy of catalyst pore size distributions from mercury porosimetry using mercury thermoporometry. Chem. Eng. Sci. 140, 291–298.
Ding, Z.L., Liu, D.S., Liu, X.M., Chen, M.Y., An, Z.S., 1989. Climate cycle of 37 times since 2.5 million. Chin. Sci. Bull. 34, 1494–1496.
Doube, M., Kłosowski, M.M., Arganda-Carreras, I., Cordelières, F.P., Dougherty, R.P., Jackson, J.S., Schmid, B., Hutchinson, J.R., Shefelbine, S.J., 2010. BoneJ: Free and extensible bone image analysis in ImageJ. Bone 47 (6), 1076–1079.
Edwards, W.M., Norton, L.D., Redmond, C.E., 1988. Characterizing Macropores that Affect Infiltration into Nontilled Soil. Soil ence Society America J. 52 (2), 483–487.
Feng, Y., Wang, J.M., Liu, T., Bai, Z.K., Reading, L., 2018. Using computed tomography images to characterize the effects of soil compaction resulting from large machinery on three-dimensional pore characteristics in an opencast coal mine dump. J. Soils Sediments 19 (3), 1467–1478.
Feng, Y., Wang, J.M., Liu, T., Bai, Z.K., Reading, L., Jing, Z.R., 2020. Three-dimensional quantification of macropore networks of different compacted soils from opencast coal mine area using X-ray computed Tomography. Soil Tillage Res. https://doi.org/10.1016/j.still.2019.104567.
Głąb, T., Ścigalska, B., Łabuz, B., 2013. Effect of crop rotations with triticale (× Triticosecale Wittm.) on soil pore characteristics. Geoderma 202, 1–7.
Hu, X., Li, Z.C., Li, X.Y., Liu, L.Y., 2016. Quantification of soilmacropores under alpine vegetation using computed tomography in the Qinghai Lake Watershed, NE Qinghai-Tibet Plateau. Geoderma 264, 244–251.
Jassogne, L., Mcneill, A., Chittleborough, D., 2010. 3D-visualization and analysis of macro- and meso-porosity of the upper horizons of a sodic, texture-contrast soil. Eur. J. Soil Sci. 58 (3), 589–598.
Kochiieru, M., Lamorski, K., Feiza, V., Feiziene, D., Volungevicius, J., 2018. The effect of soil macroporosity, temperature and water content on CO2 efflux in the soils of different genesis and land management. Zemdirbyste-Agriculture 105 (4), 291–298.
Li, Y.S., Han, S.F., Wang, Z.H., 1985. Soil water properties and its zonation in the Loess Plateau. Memoir of Northwestern Institute of Soil and Water Conservation in the Loess Plateau. Memoir of Northwestern Institute of Soil and Water. Conservation 10 (2), 1–17.
Li, D.C., Zhang, T.L., Velde, B., 2002. Application of CT analysis technology in Soil Science Research. Soils 6, 328–332.
Li, T.C., Shao, M.A., Jia, Y.H., 2016. Application of X-ray tomography to quantify macropore characteristics of loess soil under two perennial plants. Eur. J. Soil Sci. 67 (3), 266–275.
Liu, D.S., 1985. Loess and Environment. Science Press, Beijing, China (in Chinese).
Luo, L.F., Lin, H., Li, S., 2010. Quantification of 3-D soil macropore networks in different soil types and land uses using computed tomography. J. Hydrol. 393 (1–2), 53–64.
Mahmoodlu, M.G., Raoof, A., Sweijen, T., van Genuchten, M.T., 2016. Effects of Sand Compaction and Mixing on Pore Structure and the Unsaturated Soil Hydraulic Properties. Vadose Zone J. 15 (8).
Nelson, D.W., Sommers, L.E., 1982. Total carbon, organic carbon and organic matter, in Methods of Soil Analysis (Part 2, 2nd Ed.). Agronomy Monograph. 9. ASA and SSSA, Madison, WI, pp. 534–580.
Pierret, A., Capowiez, Y., Belzunces, L., Moran, C.J., 2002. 3D reconstruction and quantification of macropores using X-ray computed tomography and image analysis. Geoderma 106 (3–4), 247–271.
Poesen, J., Ingelmo-Sanchez, F., 1992. Runoff and sediment yield from topsoils with different porosity as affected by rock fragment cover and position. Catena 19 (5), 451–474.
Sander, T., Gerke, H.H., 2007. Preferential Flow Patterns in Paddy Fields Using a Dye Tracer. Vadose Zone J. 6 (1), 105.
Schneider, C.A., Rasband, W.S., Eliceiri, K.W., 2012. NIH image to imageJ: 25 years of image analysis. Nat. Methods 9, 671–675.

Sun, M., Huang, Y.X., Sun, N., Xu, M.G., Wang, B.R., Zhang, X.B., 2015. Advance in soil pore and its Influencing Factors. Chin. J. Soil Sci. 46 (01), 233–238.
Wang, M.Y., Xu, S.X., Kong, C., Zhao, Y.C., Shi, X.Z., Guo, N.J., 2019. Assessing the effects of land use change from rice to vegetable on soil structural quality using X-ray CT. Soil Tillage Res. 195, 104343.
Xu, L.Y., Wang, M.Y., Shi, X.Z., Yu, Q.B., Shi, Y.J., Xu, S.X., Sun, W.X., 2018. Effect of long-term organic fertilization on the soil pore characteristics of greenhouse vegetable fields converted from rice-wheat rotation fields. Sci. Total Environ. 631–632, 1243–1250.
Zhang, Z.B., Zhou, H., Zhao, Q.G., Lin, H., Peng, X.H., 2014. Characteristics of cracks in two paddy soils and their impacts on preferential flow. Geoderma 228–229, 114–121.
Zhao, J.B., Yue, Y.L., Du, J., 2002. Formation of Loess and division climate cycles. Journal of Desert Research 22 (1), 11–15.
Zhao, S.W., Zhao, Y.G., Wu, J.S., 2010. Quantitative analysis of soil pores under natural vegetation successions on the Loess Plateau. Sci. China Earth Sci. 2, 100–108.